Journal of Inflammation Research

Dovepress
Taylor & Francis Group

Open Access Full Text Article

ORIGINAL RESEARCH

Suppression of Inflammation by Si Miao San in Experimental Rheumatoid Arthritis Through Modulation of the AKT/ROS/Autophagy Axis

Honglin Zhang[1,*], Haixu Jiang[2,*], Qiuzhu Wei[1,*], Jie Xu[1], Zihan Zhao[1], Yuhe Sun[1], Qingyi Lu[1]

[1]School of Life Sciences, Beijing University of Chinese Medicine, Beijing, People's Republic of China; [2]School of Chinese Pharmacy, Beijing University of Chinese Medicine, Beijing, People's Republic of China

*These authors contributed equally to this work

Correspondence: Qingyi Lu, School of Life Sciences, Beijing University of Chinese Medicine, Beijing, 102488, People's Republic of China, Email lu_qingyi@126.com

Objective: Si Miao San is effective in ameliorating rheumatoid arthritis (RA) both clinically and experimentally. NETs play a fundamental role in the onset and progression of RA. The goal of this study was to explore the therapeutic effects of Si Miao San (SMS) on adjuvant-induced arthritis in mice and the regulatory mechanisms of NETs both in vivo and in vitro.

Methods: SMS decoctions were identified using LC-MS/MS analysis and TCMSP. In the adjuvant induced RA murine model, SMS decoction and methotrexate were administered orally. Disease progression was analysed by assessing arthritic scores and joint diameter, H&E staining, safranin O-fast green staining, toluidine blue staining and micro-CT analysis. The expression of NE, MPO, PAD4, LC3B, CitH3, p-AKT and p-PI3K and the production of ROS were detected using IHC, WB and IF analyses. Cytokines in the sera of the mice were detected using cytometric bead arrays. After the in vitro culture of neutrophils, NE, MPO, PAD4, LC3B, CitH3, ROS, p-PI3K and p-AKT were measured using IF and WB analyses. Autophagy was further observed with TEM.

Results: SMS decoction compounds were first identified. Compared with the model group, SMS significantly inhibited joint swelling, inflammation progression and bone destruction. The levels of NE, MPO, PAD4, CitH3, LC3B, ROS production and relative expression of p-AKT and p-PI3K in joint tissues were significantly reduced in the SMS group compared to the model group ($P < 0.05$). In vitro culture, SMS-containing serum significantly reduced the LC3B-II/LC3B-I ratio and the relative expression levels of p-AKT and p-PI3K, as well as the levels of ROS, NE, MPO, PAD4, and CitH3 compared with those in the PMA-treated group ($P < 0.05$), which was abolished by the treatment with the AKT activator SC79.

Conclusion: The SMS-induced suppression of inflammation in experimental RA occurred through the modulation of the AKT/ROS/autophagy axis.

Keywords: rheumatoid arthritis, neutrophil extracellular traps, reactive oxygen species, autophagy, protein kinase B

Introduction

Rheumatoid arthritis (RA) is an autoimmune disease that is characterized by chronic pain and joint deformities. In addition to the joints, inflammatory factors continuously activate immune cells and attack other tissues and organs, causing damage to the heart, kidneys, lungs, digestive system, eyes, skin, and the nervous system.[1,2] RA-related pain and morning stiffness lead to impairments in quality of life, such as sleep deprivation.[3] The prevalence of rheumatoid arthritis can reach as high as 1% in some areas, making it a global economic and social burden.[4]

The specific pathogenesis of RA is not fully understood; however, risk factors, such as genetics, smoking, obesity, infections, periodontal disease, and the gut microbiota, are believed to contribute to its development.[5] The diagnosis is made with the help of clinical features and laboratory investigations. RA is characterized by the presence of rheumatoid

Received: 25 February 2025
Accepted: 11 July 2025
Published: 17 July 2025

Graphical Abstract

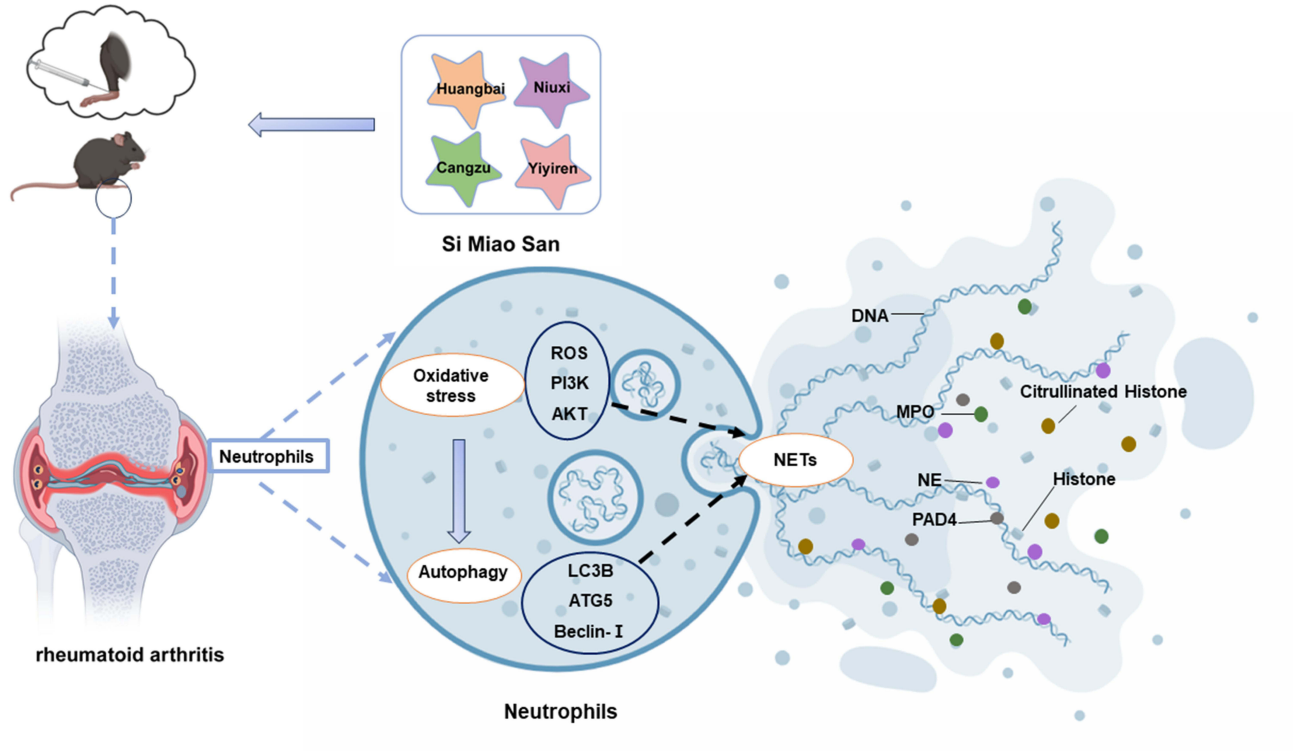

factor (RF) and other autoantibodies against posttranslationally modified proteins, such as anti-citrullinated protein antibodies (ACPAs), which form immune complexes and lead to the extended activation of immune cells.[6]

In recent years, overactivation of adaptive cells has been recognized as essential during RA progression, and the function of innate immune cells has received increasing attention. Circulating neutrophils in RA patients actively participate in the production of high levels of reactive oxygen species (ROS), cytokines, proteases with delayed apoptosis, and the formation of neutrophil extracellular traps (NETs).[7,8] During NET formation (NETosis), citrullinated histone H3 (CitH3), which is mediated by peptidyl arginine deiminase 4 (PAD4), is exposed to T cells and B cells in autoimmune diseases, leading to the emergence of autoantibodies.[9] Secreted proteases such as myeloperoxidase (MPO) and neutrophil elastase (NE) exacerbate oxidative stress and matrix degradation in joints. NET formation is induced by autophagy and ROS production.[10,11] The simultaneous expression of CitH3 has been detected, accompanied by increased autophagy during NET formation.[12] Conversely, the lack of autophagy-related 5 (Atg5), a gene encoding a protein essential for autophagosome formation, impedes NET formation.[13] During NET formation, the phosphatidylinositol-3-kinase (PI3K)/ protein kinase B (AKT) pathway is activated.[14] NADPH oxidase, PAD4, autophagy, and PI3K inhibitors significantly prevent NET formation.[13,15–17]

Conventional therapeutic strategies, including disease-modifying antirheumatic drugs (DMARDs), such as methotrexate, and other immunosuppressive agents, such as glucocorticoids, are recommended as the primary treatment for patients with RA.[18] Some recombinant biomolecules that target specific cell surface receptors or extracellular molecules have also provided another treatment option.[19] These targeted synthetic DMARDs or biological DMARDs, such as TNF-α inhibitors and Janus kinase (JAK) inhibitors, showed improved efficacy in patients who failed to achieve ideal outcomes with treatment with methotrexate (MTX) or other conventional DMARDs, but the cost and side effects significantly increased.[20] The period in which elevated autoantibodies and RA-associated risk factors are identified is

referred to as pre-RA.[21,22] According to recent clinical trials, intervention with T-cell costimulation modulation in the preclinical phase effectively reduces the progression to RA.[23,24] Traditional Chinese medicine (TCM) efficiently alleviates arthralgia in patients with RA and pre-RA. Some patented TCM medicines have been recommended as clinical treatment strategies.[25,26] Decoctions and medicines in TCM may ameliorate RA by inhibiting inflammation, regulating immune balance, and modulating the intestinal flora and metabolism.[27–29]

Si Miao San (SMS), a traditional formula documented in the medical literature in ancient China, has been used as the core component for dispelling "damp heat syndrome" in RA. It is composed of *Phellodendron amurense* (Huang Bai), *Atractylodes lancea* (Cang Zhu), *Achyranthes bidentata* (Niu Xi), and *Coix lacryma-jobi* (Yi Yiren). Different combinations of these herbal drugs are referred to as a series of classic formulas with distinct characteristics for the treatment of RA. Huang Bai and Cang Zhu are called Er Miao San, and Er Miao San with the addition of Niu Xi is called San Miao San. Experiments on rats with complete Freund's adjuvant induced arthritis (AA) showed that, compared with Er Miao San and San Miao San, Si Miao San had greater efficacy, especially in terms of bone recovery.[30] Multiomics combined with network pharmacology analysis has demonstrated its anti-inflammatory, analgesic, and immunomodulatory effects.[31] In animal experiments, SMS effectively mitigated RA progression by lowering proinflammatory cytokine levels and reducing oxidative stress.[32] Moreover, SMS has been shown to ameliorate RA-induced lung fibrosis both theoretically and experimentally.[33,34]

However, the therapeutic mechanisms of SMS in RA remain unclear owing to the multicomponent, multitarget, and multipathway nature of Chinese herbal remedies. This study focused on the underlying effects of SMS on neutrophils and the regulatory mechanism through which NET formation is modulated.

Materials and Methods

Animals

The experimental animals used in this study were provided by Beijing Vital River Laboratory Animal Technology Co., Ltd. [licence number: SCXK (jing)-2021-0006], including SPF-grade C57BL/6N mice (6–7 weeks old, weighing approximately 20 g) and SD rats (weighing approximately 250 g). The animals were housed in the specific pathogen free (SPF) experimental animal centre of Beijing University of Traditional Chinese Medicine (temperature, 22 ± 2 °C; humidity, 50 ± 5%; natural circadian rhythm) without dietary restriction. Before the start of the experiments, the mice were randomly grouped for one week of adaptive feeding.

Drugs and Chemicals

Herbs in the SMS decoctions were purchased from Beijing Tong Ren Tang Co., Ltd. They were mixed at a ratio of 1:1:1:1 and boiled for 60 min. The decoctions were filtered through gauze and concentrated to a final concentration of 1.5 g/mL. Methotrexate (MTX) was obtained from Shanghai Pharmaceutical Xinyi Pharmaceutical Co. Ltd. Antibodies against AKT (4685), p-AKT (4060), PI3K (4257), p-PI3K (4228), and β-actin (4970S) were purchased from Cell Signaling Technology (Danvers, MA, USA). Antibodies against α-tubulin (66031-1-Ig), ATG5 (10,181-2-AP), and PAD4 (17,373-1-AP) were purchased from Proteintech Group Inc. (Wuhan, HB, CHN). Antibodies against MPO (ab9535), CitH3 (ab281584), NE (ab68672), Beclin1 (ab207612), Alexa Fluor® 647 (ab150079), and HRP-conjugated goat anti-rabbit IgG (ab6721) were obtained from Abcam (Cambridge, MA, USA). Antibodies against microtubule-associated protein 1 light chain 3B (LC3B) (A19665) were obtained from ABclonal Biotechnology Co. Ltd. Phorbol 12-myristate 13-acetate (PMA) (P1585) were obtained from Sigma Chemicals (Louis, MO, USA). SC79 (305,834–79-1) and MK2206 (1,032,350–13-2) was purchased from Selleck Chemicals (Houston, USA). Stripping buffer (PS107) was purchased from Epizyme (Shanghai, China).

Mouse AA Model and Drug Treatment

The mice were then randomly divided into six groups: the normal control group (Control), the adjuvant-induced arthritis group (AA), the Si Miao San low-dose administration group (SMS-L), the Si Miao San medium-dose administration group (SMS-M), the Si Miao San high-dose administration group (SMS-H), and the MTX-treated group. Joint inflammation was induced as previously described.[35] After anaesthetization with isoflurane, 100 μL of complete Freund's

adjuvant (CFA) was injected into the ankle joint cavity of the left hindfoot of C57BL/6 mice.[35] From the 4th to the 31st day after CFA immunization, the mice in the SMS-L, SMS-M and SMS-H groups were administered SMS decoction at concentrations of 6.24, 12.48, and 24.96 g/(kg·d), respectively. The dosage was calculated according to previous publications.[32,33] The mice in the MTX group were orally administered MTX every two days at a concentration of 1.73 mg/kg. On the 4th day after CFA injection, the ankle joint diameters were recorded every three days, and the joints were scored according to a five-grade scoring system.[36]

SMS Mass Spectrometry Detection

LC–MS/MS analysis was performed using an Agilent ultrahigh-performance liquid chromatography (HPLC) 1290 UPLC system. A Q Exactive Focus mass spectrometer coupled with Xcalibur software (Thermo Fisher Scientific, Waltham, Massachusetts, USA) was used to obtain MS and MS/MS data in the IDA acquisition mode.

Histopathology Analysis

Joint paraffin sections were prepared as described previously.[35] Haematoxylin and eosin (H&E) staining, toluidine blue staining, safranin O-fast green staining, periodic acid-Schiff staining (PAS) and TUNEL staining were performed according to standard procedures. Pathological changes in the ankle joints of the mice were observed and scored according to specific criteria.[37]

Immunohistochemistry (IHC) Analysis

After dewaxing and hydration, the tissue sections were incubated with 0.05% Triton X-100 at 37 °C for 30 min for permeabilization. After rinsing three times with PBS, 3% H_2O_2 was used to remove endogenous peroxidase. Antigen retrieval was performed as previously described.[38] After blocking, the sections were incubated with the primary antibody against the target protein at an appropriate concentration at 4 °C overnight and then with the secondary antibody at 37 °C for 30 min. The target proteins were finally developed with 3,3'-diaminobenzidine (DAB) and analysed with ImageJ software (National Institutes of Health, Bethesda, MD, USA) by quantifying the IOD of the positive area.

Immunofluorescence Assays (IFAs) of Tissue Sections

An opal 3-plex anti-Rb manual detection kit (Cat#: NEL840001KT, Akoya Biosciences, Co., Ltd, Delaware, USA) was used to simultaneously detect the expression of target proteins. All the experiments were performed in accordance with the guidelines. Finally, the nuclei were counterstained with DAPI. The slides were mounted and imaged using a confocal microscope. The fluorescent signals were analysed using ImageJ software (National Institutes of Health, Bethesda, MD, USA).

Microcomputed Tomography (Micro-CT) Analysis

Mouse ankles were collected and fixed in paraformaldehyde, and microcomputed tomography (micro-CT) specimens were scanned using a Bruker Micro-CT Skyscan 1276 system (Bruker, Germany). Analyses were performed using the manufacturer's evaluation software. Reconstruction was performed using NRecon (Brucker, version 2.2.0.6, Bruker, Germany), and 3D images were obtained from 2D images using a method based on the grayscale original image distance transform (CTvox, version 3.3.0.0, Bruker, Germany). 2D and 3D analyses were performed using CT Analyzer software (version 1.20.8.0, Bruker, Germany). ROIs were analysed using CT Analyzer software (version 1.20.8.0, Bruker, Germany). The bone volume (BV), bone volume density (BV/TV), and bone surface area (BS) were calculated using CT Analyzer software (Bruker, Germany) to evaluate the morphology, microarchitecture, and bone quality of representative mice.

Cytometric Bead Arrays of Serum Cytokines

The experimental procedures were performed according to the instructions provided for the cytometric bead array (CBA) kit (Cat#: 560485, BD Biosciences, New Jersey, USA). Standards were prepared according to the manufacturer's instructions. Th1/Th2/Th17 capture beads (40 μL) were added to each well of the 96-well plate. Standard diluents or

samples (50 μL) were added, followed by 40 μL of detection reagent. The 96-well plate was sealed with a membrane and incubated at room temperature in the dark for 2 h. After washing, the beads were transferred to a new 96-well plate and were then subjected to fluorescence-activated cell sorting (FACS) and analysed using FCAP Array software (BD Biosciences, New Jersey, USA).

Preparation of Drug-Containing Serum

SD rats were randomly divided into normal control and SMS administration groups. SMS was orally administered at a dosage of 34.944 g/(kg·d). The control group was given water for 7 consecutive days. After the last gavage, blood was collected from the abdominal aorta, and the serum was collected after centrifugation at 4 °C and 3000 rpm for 20 min. After heating at 57 °C for 30 min, the SMS-containing and control sera were then filtered through a 0.22 μm diameter microporous membrane and stored at - 80 °C for future use.

Recruitment, Isolation and Culture of Mouse Peritoneal Neutrophils

Peritoneal neutrophils were isolated as previously described.[39] Briefly, after peritoneal injection of 10% proteose peptone (prepared in saline) twice, the cells were recovered and resuspended in the cell culture medium. Neutrophils were isolated using Percoll (Cat#: P8370, Solarbio, Beijing, China) and cultured under different treatments.

CCK8 Assay

A Cell Counting Kit 8 (CCK8) was purchased from Beijing Aoqing Biotechnology Co., Ltd. (Cat#: AQ308). Primary neutrophils were inoculated into 96-well plates as previously described.[35] Different concentrations of SMS-containing serum were added and cultured for 4 h. CCK8 solution (10 μL/well) was added to each well and incubated for 1 h. The absorbance was measured at 450 nm using a microplate reader.

Immunofluorescence Assays in Cell Culture

Neutrophils (1×10^6) were seeded in a laser confocal culture dish and cultured with or without PMA or SMS-containing sera. This procedure was performed as previously described.[35] In brief, after fixation and permeabilization, the cells were blocked and incubated with primary antibodies at 4 °C overnight. The next day, after rinsing with PBS, secondary antibodies were added, and the cells were incubated with DAPI. A laser confocal microscope was used to observe the staining, and photographs were taken. The fluorescence intensity of the target protein and the area of the nucleus were analysed using ImageJ software (National Institutes of Health, Bethesda, MD, USA).

Detection of Reactive Oxygen Species From Periarticular Tissue and Cell Culture

The joint tissues were dissociated using a skeletal muscle dissociation kit (Cat#:130–098-305, Miltenyi Biotec, Cologne, Germany). The supernatant was discarded by centrifugation at 800 × g for 10 min. The pellets were subsequently resuspended in 1 mL of PBS and counted. The DCFH-DA probe from an ROS assay kit (Cat#: E004-1-1, Nanjing Jiancheng Bioengineering Institute, Nanjing, China) was then added and incubated with the cells at 37 °C for 40 min in the dark. FITC fluorescence was detected by fluorescence-activated cell sorting (FACS), as suggested by the guidelines.

For the production of ROS from neutrophils in vitro, 1×10^6 neutrophils were seeded in a laser confocal dish and incubated with diluted DCFH-DA after different treatments. The cells were then washed three times with serum-free cell culture medium to remove DCFH-DA from the supernatant. The fluorescence intensity was observed directly using a laser confocal microscope.

Total Protein Extraction From Mouse Tissues and Neutrophils

Radioimmunoprecipitation assay lysis buffer (RIPA) was purchased from Solarbio (Beijing, China). Periarticular tissues were collected and lysed using a tissue homogenizer after the addition of RIPA complete buffer (with 1 mM PMSF). The tissue samples were subsequently incubated on ice for 15–30 min to facilitate lysis and the supernatants were collected after centrifugation at 12,000 rpm for 10 min at 4 °C. After the addition of loading buffer, the protein samples were heated at 95 °C for 5 min and stored for future use.

Isolated neutrophils were cultured in six-well plates at 5×10^6 cells per well and labelled as the NC, NC + PMA, SMS, SMS+PMA, and SMS+PMA+SC79 groups. After four-hour treatment, the supernatant and the neutrophils at the bottom of the wells were collected. After centrifugation, RIPA buffer (with 1 mM PMSF) was added to the pellets. The lysates were centrifuged at 12,000 × g for 10 min, and the supernatant was collected. After the addition of loading buffer, the protein samples were heated at 95 °C for 5 min.

Western Blot Analysis

Protein samples were separated by sodium dodecyl sulfate–polyacrylamide gel electrophoresis (SDS–PAGE) and transferred to polyvinylidene fluoride (PVDF) membranes. After being blocked with 3% bovine serum albumin (BSA) in TBST buffer (Tris-buffered saline with 0.05% Tween-20) for 2 h, the membranes were incubated with primary antibodies overnight at 4 °C. The membranes were then incubated with an HRP-conjugated secondary antibody for 1 h at room temperature. Proteins were detected with ECL reagent (Cat#: 36208ES, Yeasen Biotechnology Co., Ltd., Shanghai, China) and visualized. The grey values of the target bands were subsequently analysed using ImageJ software (National Institutes of Health, Bethesda, MD, USA), and the results were recorded. After WB detection, the membrane was stripped and re-probed with another antibody.

Transmission Electron Microscopy for Detection of Neutrophils

After the different treatments were performed in vitro, the cell culture medium was replaced with 2.5% glutaraldehyde, and the cells were fixed for 24 h. The glutaraldehyde solution was then removed, and the cells were washed with PBS for 6 h. Subsequently, the cells were postfixed with 1% osmium tetroxide. Dehydration was performed using a graded ethanol series, and the cells were stained with uranyl acetate dissolved in 70% ethanol during dehydration. The dehydrated samples were then infiltrated with a 1:1 mixture of propylene oxide and epoxy resin and embedded in pure epoxy resin. The embedded samples were polymerized in an oven at 45 °C for 12 h and then at 72 °C for 24 h. After curing, the resin blocks were trimmed, and ultrathin sections (approximately 70 nm thick) were prepared. Sections were collected on copper grids and stained with lead for imaging. The final images were captured using a transmission electron microscope (JEOL Ltd., Tokyo, JEM-1400).

Molecular Docking

The components of SMS were acquired from the Traditional Chinese Medicine Systems Pharmacology Database and Analysis Platform (TCMSP, http://tcmspw.com/tcmsp.php). The active compounds were filtered based on oral bioavailability (OB) ≥ 30% and a drug-likeness (DL) ≥ 0.18. The corresponding targeted genes of the active ingredients were also retrieved and compared with the names in the UniProt database (https://www.uniprot.org/) to ensure unique gene nomenclature. Cytoscape 3.9.1 software (Cytoscape Consortium) was used to create the network diagram of herbs, active ingredients and targeted genes, from which the "Degree" values were calculated based on the number of edges directly connecting a node to other nodes. The 3D structures of the small molecule compounds (Degree≥30) were retrieved from the PubChem database (https://pubchem.ncbi.nlm.nih.gov/). The molecular structures of the agents and the human AKT protein (Protein Data Bank ID: 1GZO) were subsequently constructed and preprocessed using Autodock Tools 2.4.6 (The Scripps Research Institute, California, USA). Molecular docking was performed, and the docking results were visualized using PyMOL 3.1 (Schrödinger, LLC, New York, USA).

Statistical Analysis

Statistical analyses were performed using SPSS Statistics 20.0 (IBM, Armonk, New York) and GraphPad Prism 7 software (Insightful Science, San Diego, California). The data were presented as the means ± standard deviations (SDs). For normally distributed data, one-way analysis of variance (ANOVA) was used for comparisons among multiple groups, and least significant difference (LSD) tests were used for pairwise comparisons. Nonnormally distributed data were analysed using nonparametric tests. Statistical significance was defined as $P < 0.05$.

Results

Improvement of Arthritis in RA Mice by Si Miao San

The chemical fingerprinting results of the SMS decoctions (Supplementary Figure 1) identified specific compounds listed in Supplementary Tables 1 and 2. The active ingredients include quercetin, wogonin, berberine, palmatine and kaempferol, which were also identified as the principal active components of SMS in other studies.[40–42]

The AA model was established on Day 0. Treatment with high, medium, and low doses of SMS and MTX was initiated on Day 4. Joint diameters and scores were recorded every 3 days (Figure 1A). Statistical analysis revealed that the joint scores and diameters in the high-dose SMS and MTX groups were significantly lower than those in the AA group. No significant differences were observed between the low- and medium-dose SMS groups and the AA group (Figure 1B and C). Compared with the mice in the control group, the mice in the model group presented severe symptoms, such as joint swelling, which was significantly alleviated by high doses of SMS and MTX (Figure 1D). However, no significant difference in body weight was observed between the groups (Figure 1E). The splenic index was calculated using the following formula: Splenic index = spleen weight (g)/body weight (g). SMS-H and MTX significantly reduced the spleen indices of the AA mice (Figure 1F). H&E staining revealed typical pathological states in the ankle joints of the AA group, including synovial cell hyperplasia and inflammatory cell exudation within the joint cavities. The degree of inflammatory cell infiltration was visualized using H&E staining, and the joints of arthritic mice were subsequently scored on an inflammation scale ranging from 0–4. In contrast, these pathological states were mitigated in the SMS-H and MTX groups, as reflected by decreased histological scores. However, no significant changes in the local ankle joint pathological state were observed between the SMS-L and SMS-M groups and the AA group ($P > 0.05$) (Figure 1G and H).

PAS staining (Supplementary Figure 2) and TUNEL staining (Supplementary Figure 3) of liver and kidney tissues revealed no damage to the liver or kidneys in any of the groups, indicating the safety of SMS when administered at different dosages.

Subsequently, relevant pathological tests were performed on the ankle joints in each group. Safranin O-fast green and toluidine blue staining demonstrated that cartilage damage in the ankle joints was effectively protected in the high-dose SMS and MTX groups compared with the AA group (Figure 2A-C). Furthermore, the bone mineral densities of the mice in the control, AA, SMS-H, and MTX groups were analysed using micro-CT, which confirmed that the bone surface erosion induced by joint inflammation was alleviated by SMS-H and MTX treatment (Figure 2D and E). The changes in the serum levels of inflammatory cytokines indicated that the TNF-α and IL-6 levels were significantly elevated in the AA group compared with those in the control group, and were markedly reduced by SMS-H and MTX treatment (Figure 2F and G).

Local NET Formation in Joints Was Inhibited by SMS

Increasing evidence indicates that neutrophils play a significant role in regulating both innate and adaptive immunity[43] and that inhibiting NET production can ameliorate RA symptoms.[44–46] SMS has been reported to decrease MPO activity in the joint tissues of mice with gouty arthritis.[47] To explore whether SMS alleviated RA by regulating NET formation, the activity of MPO, an essential enzyme of neutrophils, was first detected (Figure 3A and B). PAD4 was also detected using IHC (Figure 3C and D). Compared with the control group, the AA group presented significantly elevated levels of MPO and PAD4, which were reduced by high-dose SMS. Additionally, immunofluorescence analysis of NE and CitH3 was performed to confirm NET formation (Figure 3E–G). High doses of SMS and MTX significantly reduced CitH3 and NE protein expression, suggesting that SMS inhibits NET production in mice with RA.

The PI3K/AKT Signalling Pathway, ROS Production, and Autophagy Generation Were Inhibited by SMS in vivo

Neutrophil activation leads to increased ROS production, which in turn induces NET formation through mechanisms such as DNA damage and the NADPH oxidase complex.[48,49] ROS not only act as antimicrobial effectors but also serve as signalling molecules that regulate nuclear factor kappa-B (NF-kB) transcriptional activity and promote NET

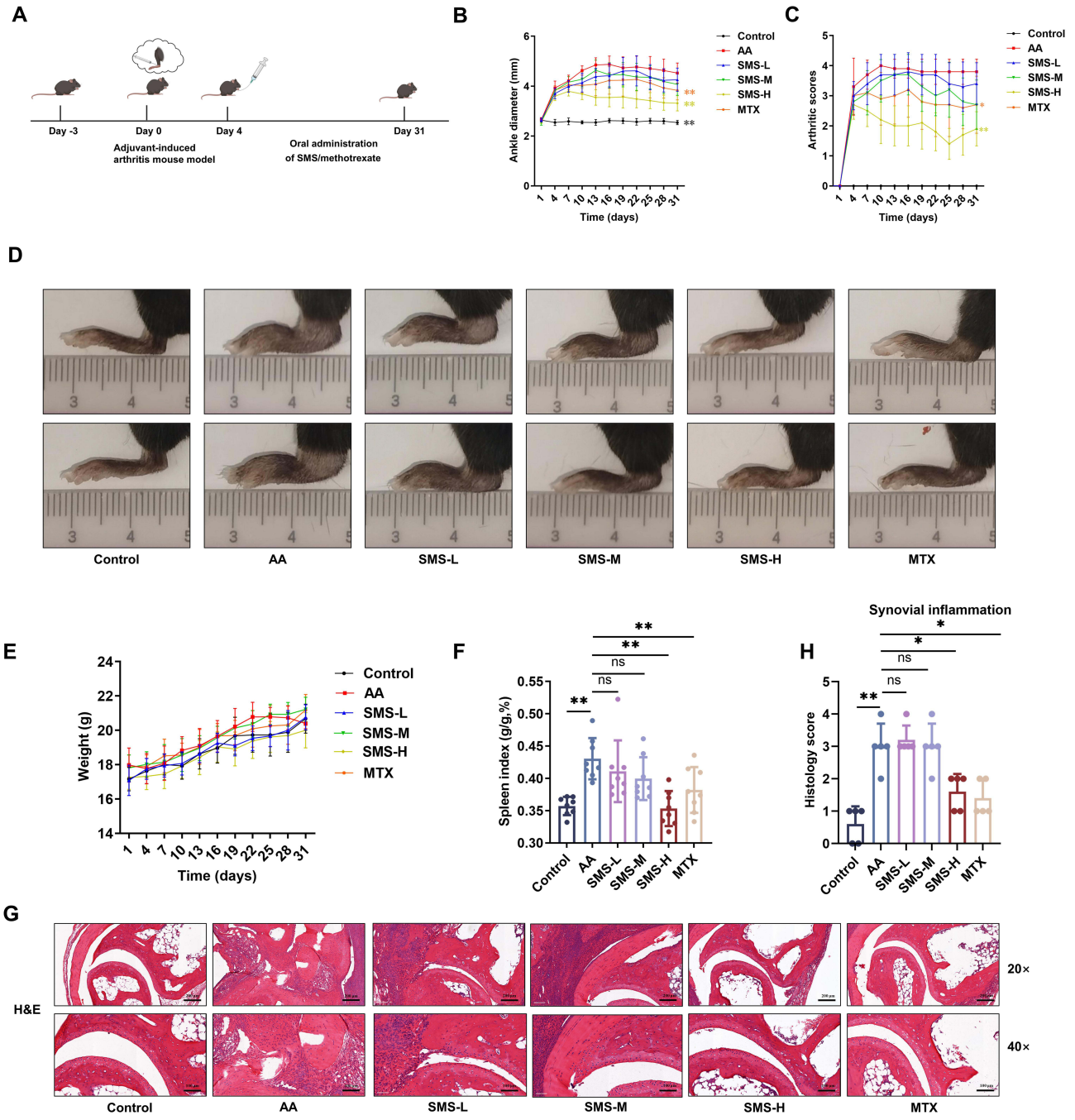

Figure 1 SMS attenuated the severity of arthritis in AA mice. (**A**) Schematic representation of the animal experiment. (**B**) Joint swelling was assessed by measuring the ankle joint diameter ($n = 8$). (**C**) Arthritis severity was graded on a scale of 0–4. (**D**) Representative images of arthritic paws from each group at the end of the experiments. (**E**) Changes in the body weights of the mice ($n = 8$). (**F**) Mouse spleen index ($n = 8$). (**G**) H&E images. Scale bars, 100 and 200 μm. (**H**) Histological scores ($n = 5$). The values are presented as the means ± SDs. *$P<0.05$, **$P<0.01$, $^{ns}P > 0.05$.

production. Furthermore, activation of the PI3K/AKT signalling pathway enhances ROS production, contributing to increased NET generation and thus playing a crucial role in neutrophil function.[50,51]

As shown in Figure 4A and B, SMS-H and MTX significantly reduced the ROS levels in the cells of the joints. The elevated ROS levels in the peri-ankle tissues of the mice in the AA group were consistent with the increased NET formation in the AA group. The levels of phosphorylated AKT and PI3K in the ankle joints were examined by WB analysis (Figure 4C-F). SMS treatment significantly reduced the phosphorylation levels of AKT and PI3K, indicating the inhibition of the PI3K/AKT signalling pathway by SMS. In addition, ROS are known to influence autophagy processes.[52]

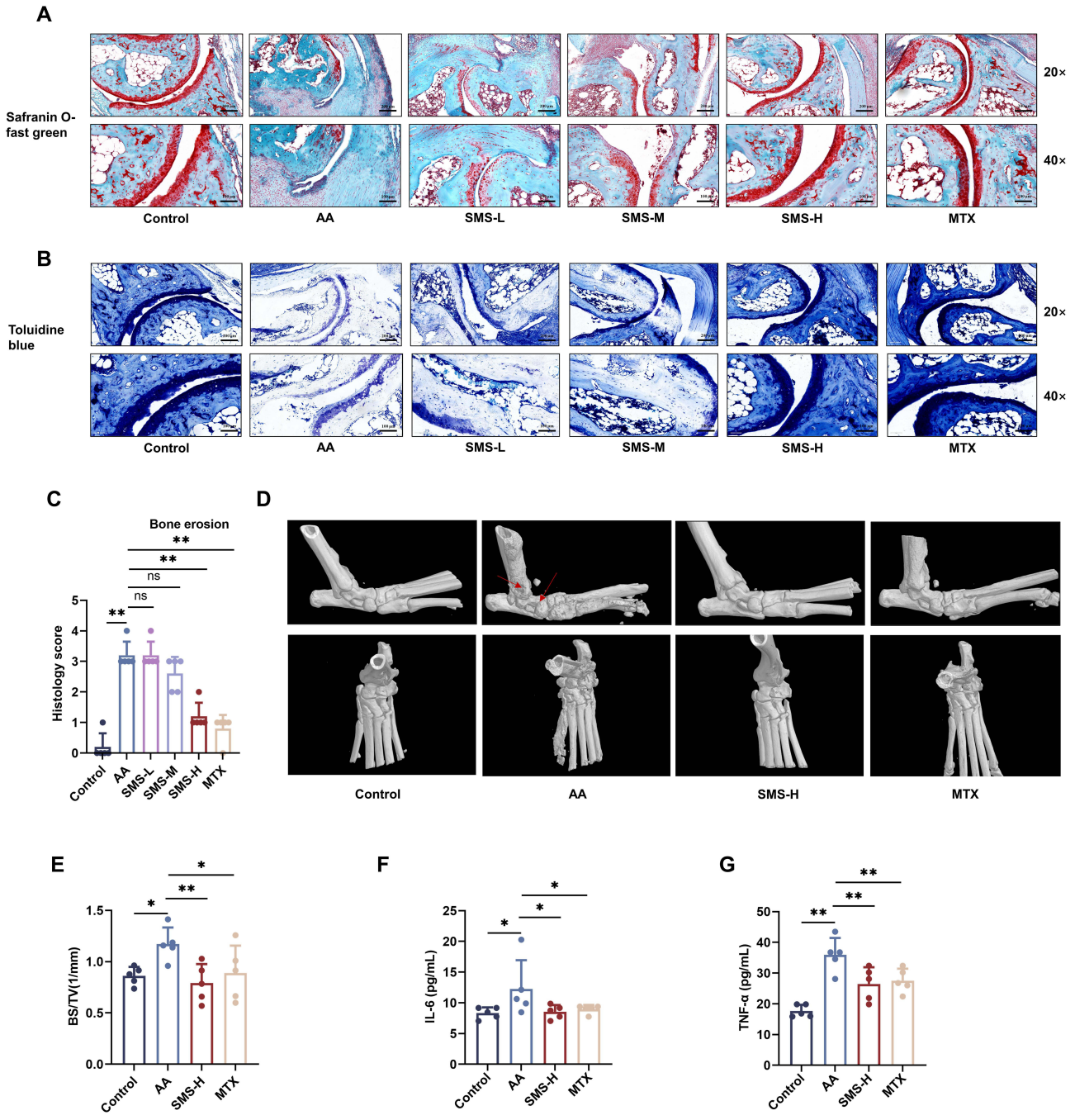

Figure 2 Bone destruction in mice with RA was ameliorated by SMS. Representative joints with (**A**) safranin O-fast green staining and (**B**) toluidine blue staining. Scale bars, 100 and 200 μm. (**C**) Histological scores (n = 5). (**D**) Representative micro-CT images of the mice. The red arrows indicate bone damage. (**E**) BV/TV of each group (n = 5). (**F**) IL-6 concentration in the serum of each group (n = 5). (**G**) TNF-α concentration in the serum of each group (n = 5). The values are presented as means ± SDs. *P<0.05, **P<0.01, ^{ns}P > 0.05.

Enhanced neutrophil autophagy has been observed in patients,[53,54] and the inhibition of autophagy has been reported to reduce NET production.[55,56] To assess the level of autophagy in RA, the expression of LC3B in mouse ankles was analysed using IHC. As shown in Figure 4G and H, high-dose SMS treatment greatly reduced LC3B expression in the ankle joints of AA mice. In summary, SMS appears to alleviate RA by suppressing the PI3K/AKT signalling pathway, reducing ROS production, attenuating autophagy in peri-ankle tissues, and reducing NET formation.

https://doi.org/10.2147/JIR.S524871

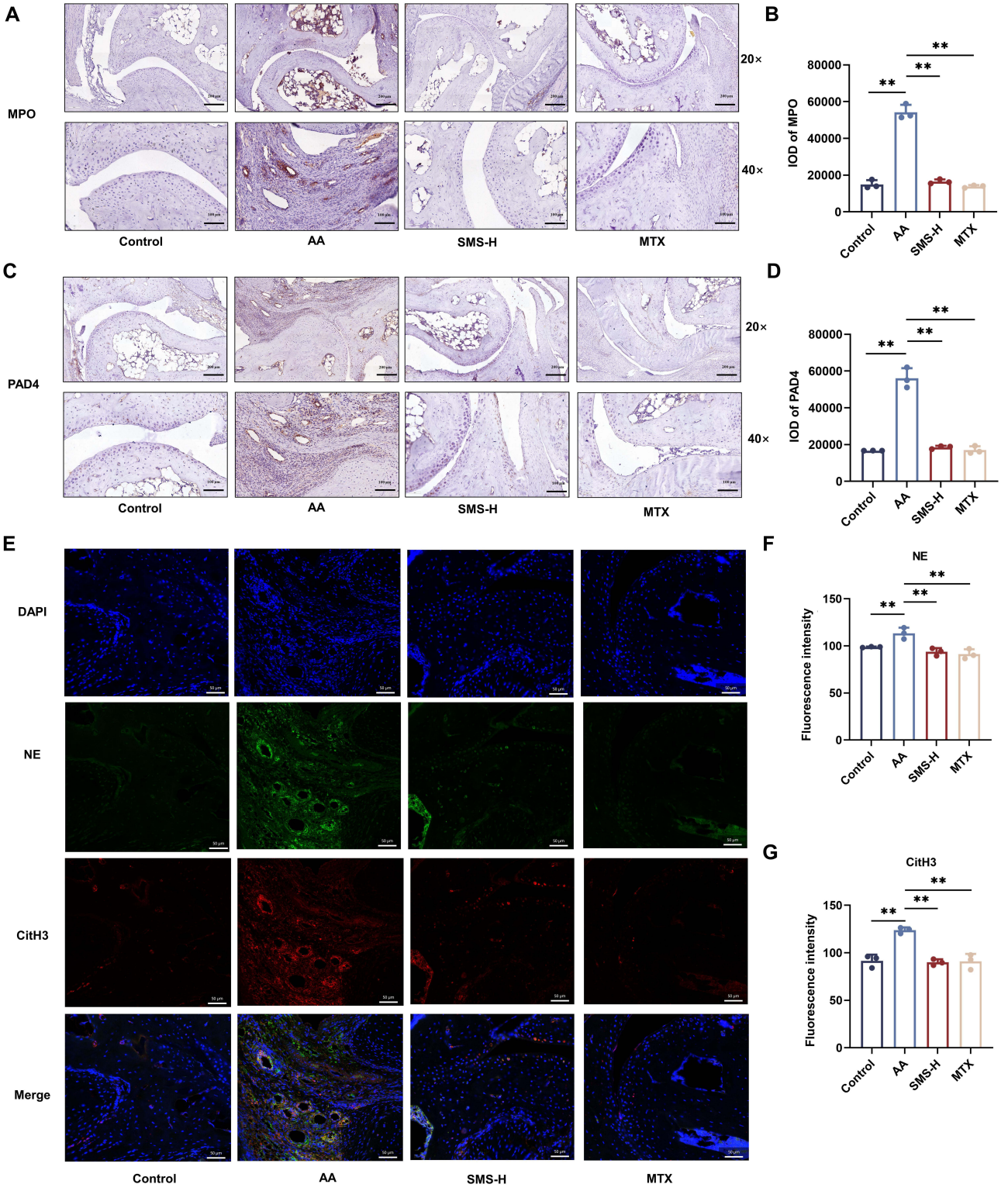

Figure 3 SMS inhibited local NET formation in joints. (**A**) IHC was used to assess MPO protein expression in mouse ankle joints. Scale bars, 100 and 200 μm. (**B**) Quantitative analysis of (**A**) (*n* = 3). (**C**) IHC was used to assess PAD4 protein expression in mouse ankle joints. Scale bars, 100 and 200 μm. (**D**) Quantitative analysis of (**C**) (*n* = 3). (**E**) Immunofluorescence analysis was used to detect the expression levels of CitH3 and NE proteins in mouse joints. (**F**) Quantitative analysis of NE (*n* = 3). (**G**) Quantitative analysis of CitH3 (*n* = 3). The values are presented as the means ± SDs. **$P<0.01$.

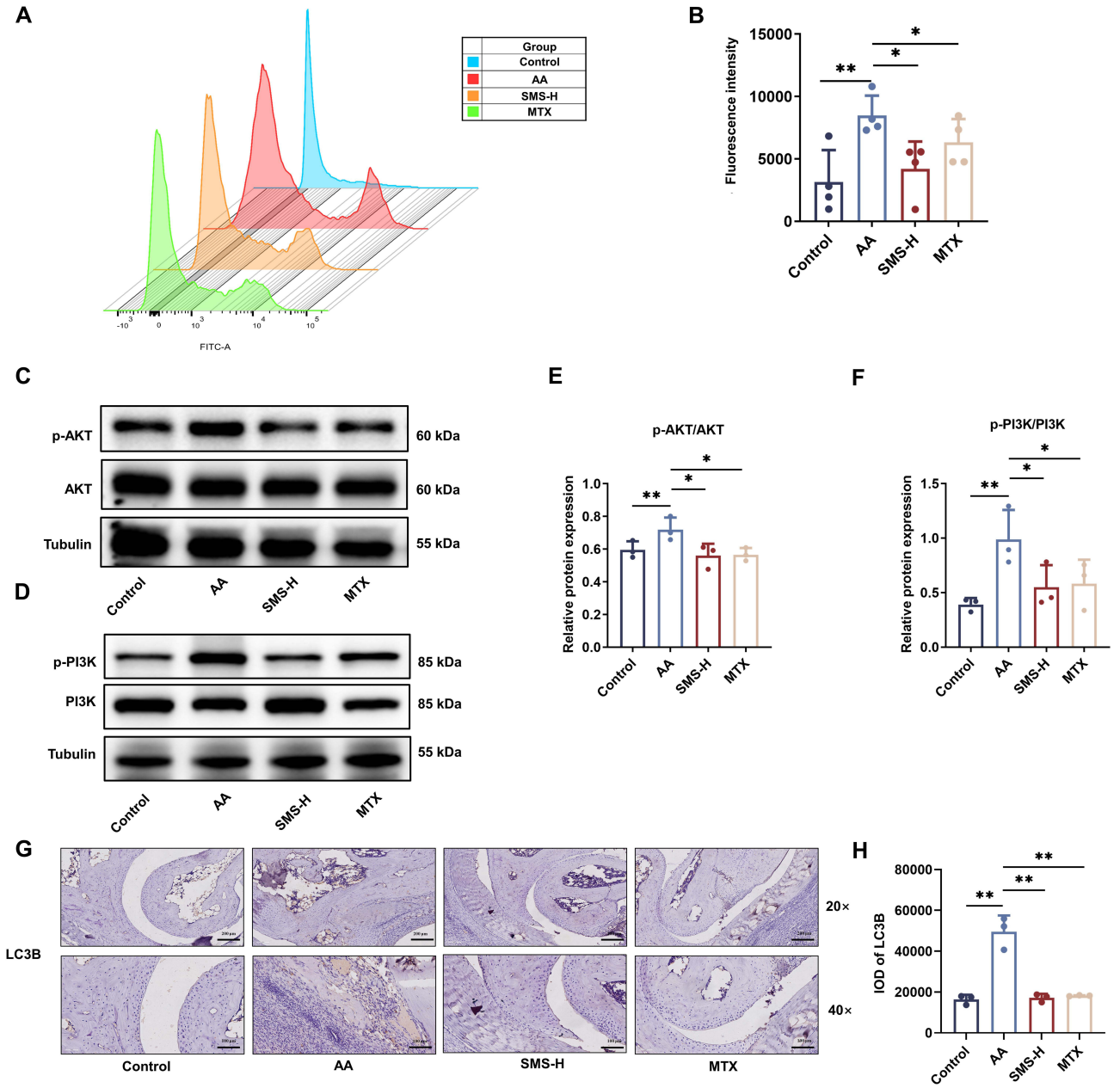

Figure 4 SMS inhibited local NET formation in joints through PI3K/AKT/ROS/autophagy axis. (**A**) FACS analysis of ROS production. (**B**) Quantitative analysis of (A). (**C**) WB analysis of the expression of p-AKT and AKT in periarticular muscle tissues. (**D**) WB analysis of the expression of p-PI3K and PI3K in periarticular muscle tissues. (**E**) Quantitative analysis of p-AKT in (**C**) (n = 3). (**F**) Quantitative analysis of p-PI3K in (**D**) (n = 3). (**G**) IHC analysis of LC3B protein expression. Scale bars, 100 and 200 μm. (**H**) Quantitative analysis of LC3B in G (n = 3). The values are presented as means ± SD. *P<0.05, **P<0.01.

Effects of SMS-Containing Serum on the PI3K/AKT Signalling Pathway and NET Formation in Neutrophils in vitro

Our previous reports revealed that the activation of PI3K/AKT leads to the autophagy of neutrophils.[35,57] MK2206, an AKT inhibitor, was reported to inhibit ROS production and NET formation.[58] MK2206 suppressed ROS production (Supplementary Figure 4A and 4B), as well as NET formation and autophagy (Supplementary Figure 4C-F), indicating that inhibition of AKT has led to the regulation of ROS/autophagy/NETs axis.

To further investigate the effect of SMS on NET production, primary neutrophils from the peritoneal cavities of mice were used for in vitro experiments. CCK8 assays were performed to determine the concentration of drug-containing serum in the cell culture medium. The addition of 1% serum of control rats and SMS-containing serum had no significant

https://doi.org/10.2147/JIR.S524871

effect on cell viability (Supplementary Figure 5). NET formation was induced in vitro using PMA and the effects of SMS-containing serum were examined. SC79, an AKT activator that promotes AKT phosphorylation, was used to assess the involvement of the PI3K/AKT pathway in this process. As expected, PMA significantly increased p-AKT levels in neutrophils cultured with serum from control rats, whereas SMS-containing serum reduced AKT phosphorylation. SC79 treatment further increased AKT phosphorylation (Figure 5A and B). Similar trends were observed for p-PI3K levels (Figure 5C and D). Cellular immunofluorescence (IF) analysis revealed that PMA stimulation elevated the expression of CitH3 (Figure 5E and I), MPO (Figure 5F and J), NE (Figure 5G and K), and PAD4 (Figure 5H and L) in neutrophils in the control serum, whereas significant reductions were observed following treatment with SMS-containing serum. SMS-containing serum also significantly reduced the neutrophil nuclear area after PMA stimulation (Figure 5M–P). However, SC79 eliminated the suppressive effect of SMS on NET formation.

Neutrophil ROS Production and Autophagy Were Inhibited by SMS-Containing Serum in vitro

PMA activates protein kinase C, which, in turn, activates the NADPH oxidase complex, leading to increased ROS production.[59] Figure 6A and B shows that ROS significantly increased after PMA stimulation in vitro, whereas SMS-containing serum effectively reduced ROS generation. SMS also decreased the expression levels of autophagy-associated protein 5 (ATG5), Beclin-1, and LC3B II (Figure 6C-F). Reduced LC3B levels were also observed by IF (Figure 6G and H). Additionally, autophagosomes in neutrophils were examined using TEM. PMA stimulation increased autophagosome formation in neutrophils, which was subsequently reduced by SMS treatment (Figure 6I). The inhibition of autophagy by SMS-containing serum corresponded with reduced NET formation, which is consistent with the finding that the inhibition of autophagy prevents intracellular chromatin disaggregation, thereby inhibiting the PMA-stimulated formation of NETs in neutrophils.[60] The addition of the AKT activator SC79, which activates the AKT signalling pathway, further increases ROS production and autophagy in neutrophils and abolishes the inhibitory effect of SMS serum on ROS and autophagy, indicating that SMS regulates ROS and autophagy by inhibiting the activation of AKT.

Network pharmacology analysis and molecular docking were utilized to explore the potential direct effect of SMS on AKT. As shown in Supplementary Figure 6, the four herbs of SMS contained 41 active ingredients, corresponding to 228 potential targeted proteins, which included AKT. The top 10 active ingredients according to "Degree" value are listed in the Supplementary Table 3. Wogonin, berberine, kaempferol, palmatine and quercetin were also identified by LC–MS/MS analysis. Their binding energies to AKT were calculated and are listed in Supplementary Table 4. Wogonin, berberine and palmatine were predicted to bind more strongly to AKT (< –5 kcal/mol), and the docking results are shown in Supplementary Figure 7.

Discussion

The goal of RA treatment is to achieve remission.[4] Despite infections and other side effects, the combination treatment strategy can successfully mitigate arthralgia and deformity in most patients with RA. This challenge has been proposed for some patients whose symptoms have not fulfilled the diagnostic criteria or whose disease progression is difficult to ameliorate with existing drugs.[4] TCM has been used to treat patients with RA and pre-RA in China for thousands of years. As a classic formula used in clinical treatment, SMS provides new insights into intervention targets in RA progression.

Inflammation and bone destruction are the most important pathological changes associated with RA. In this study, H&E staining and toluidine blue staining indicated that a high dose of SMS could alleviate inflammatory cell infiltration and cartilage destruction in the ankle joints of patients with RA. Micro-CT confirmed the bone-protective effects of SMS. Notably, SMS has been shown to exert osteogenic effects on osteoblasts in vitro, which further accounts for the bone protection induced by SMS in RA.[61]

Neutrophils play important roles in the development of autoimmune diseases. Activated neutrophils in rheumatoid arthritis drive inflammation by producing various cytokines, ROS, and NETs.[45] NETs significantly enhance the inflammatory response in RA by exposing autoantigens to adaptive systems and by inducing the production of IL-6,

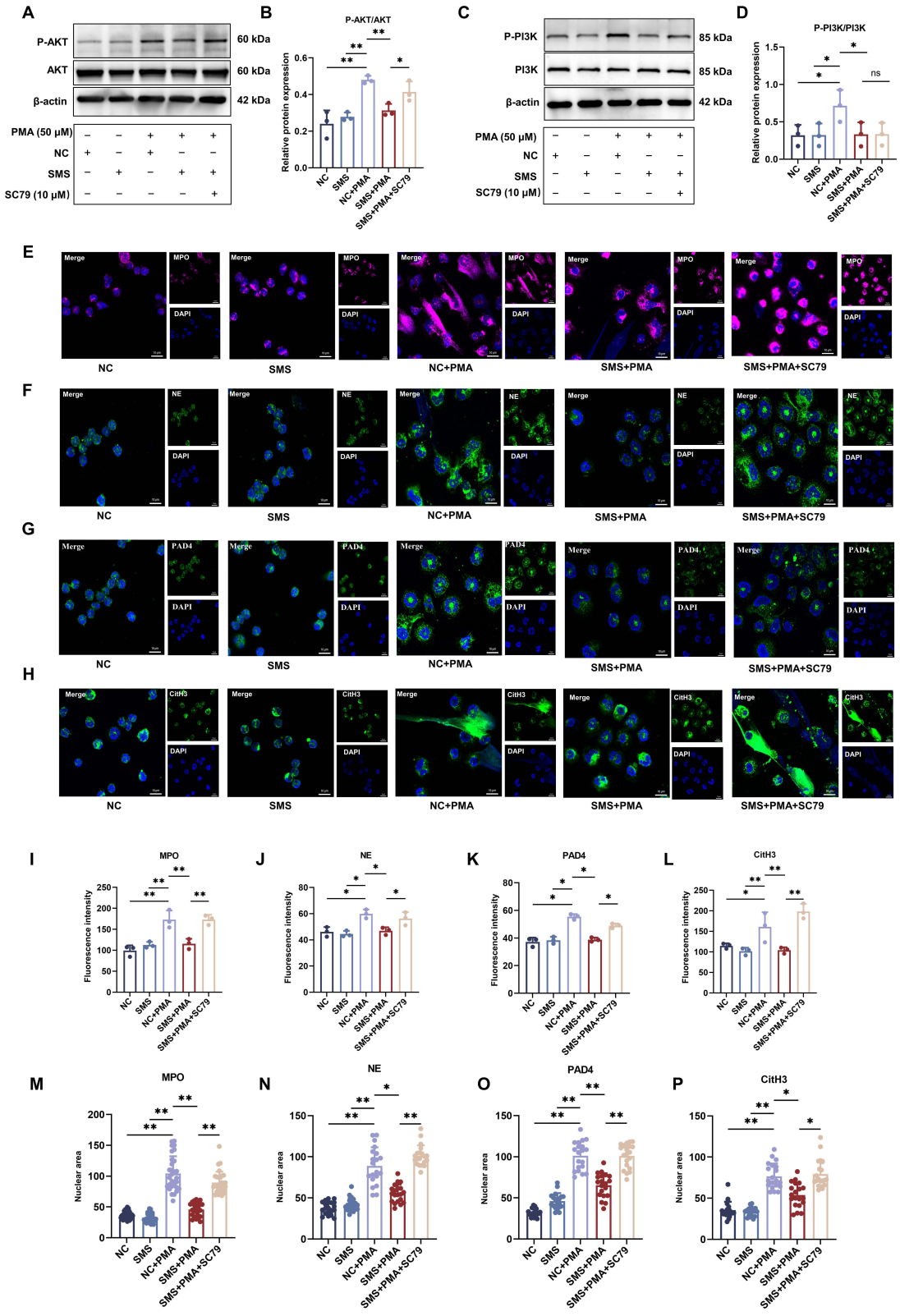

Figure 5 SMS inhibited the PI3K/AKT signalling pathway and NET production in vitro. Neutrophils extracted from the peritoneal cavity of mice were subjected to different interventions in the following groups: NC, SMS, NC+PMA, SMS+PMA, and SMS+PMA+SC79. (**A**) WB analysis of the expression of p-AKTand AKT in the neutrophils of each group. (**B**) Quantitative analysis of the relative expression of p-AKT in (A). (**C**) WB analysis of the expression of p-PI3K and PI3K in the neutrophils of each group. (**D**) Quantitative analysis of the relative expression of p-PI3K in (C). (**E**) IF analysis of MPO expression. (**F**) IF analysis of NE expression. (**G**) IF analysis of PAD4 expression. (**H**) IF analysis of CitH3 expression. (**I**) Quantitative analysis of MPO in (**E**) (n = 3). (**J**) Quantitative analysis of NE in (**F**) (n = 3). (**K**) Quantitative analysis of PAD4 in (**G**) (n = 3). (**L**) Quantitative analysis of CitH3 in (**H**) (n = 3). (M)Neutrophil nuclear area of (**E**) (n = 20). (**N**) Neutrophil nuclear area of (**F**) (n = 20). (**O**) Neutrophil nuclear area of (**G**) (n = 20). (**P**) Neutrophil nuclear area of (**H**) (n = 20). The values are presented as the means ± SDs. *P<0.05, **P<0.01, ^{ns}P > 0.05.

https://doi.org/10.2147/JIR.S524871

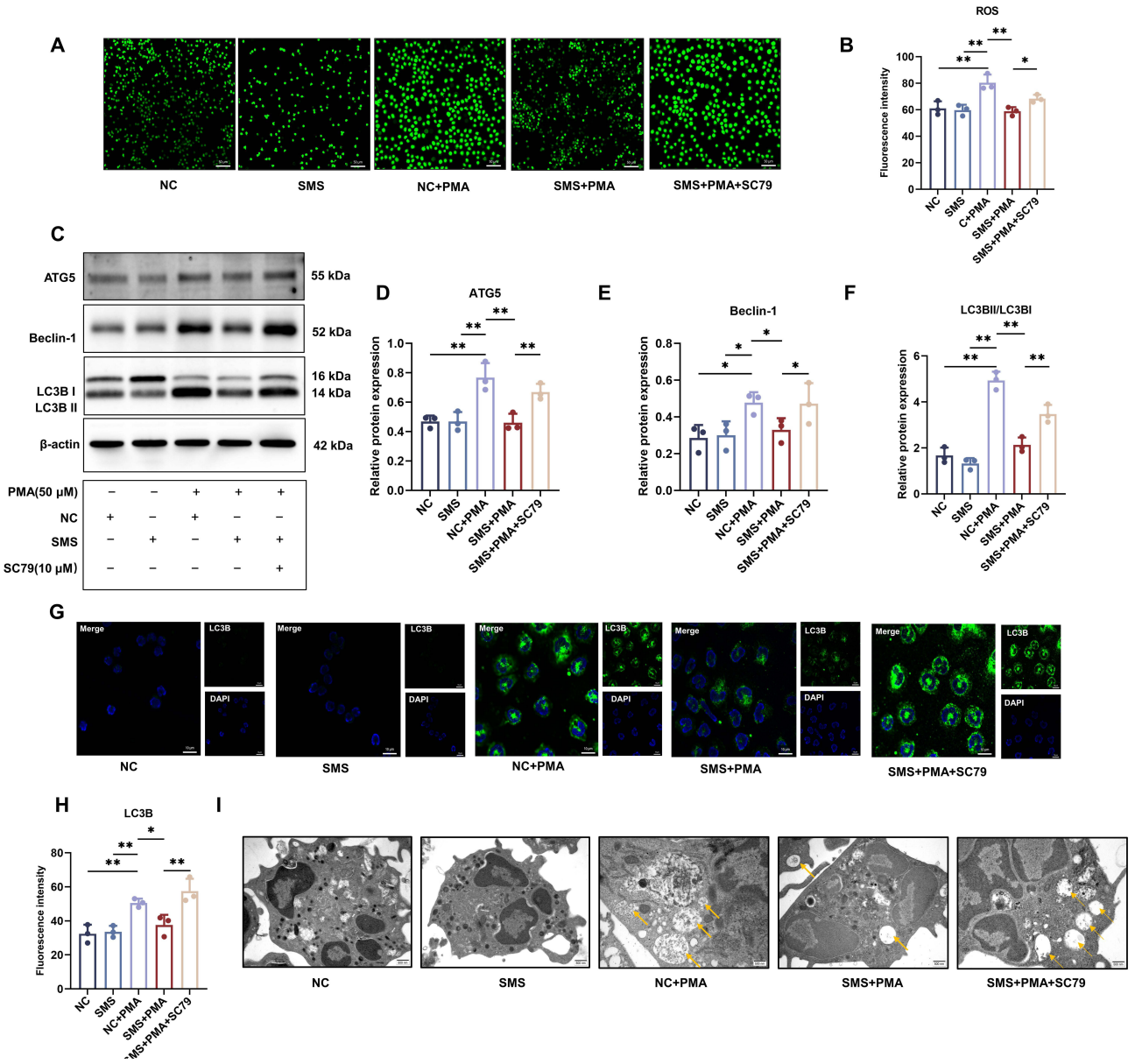

Figure 6 SMS inhibited ROS production and autophagy through AKT signalling in vitro. Neutrophils extracted from the peritoneal cavity of mice were subjected to different interventions in the following groups: NC, SMS, NC+PMA, SMS+PMA, and SMS+PMA+SC79. (**A**) IF images of neutrophils from each group after being stained with DCFH-DA for 4 h. (**B**) Quantitative analysis of ROS in (**A**) (*n* = 3). (**C**) WB analysis of the expression of ATG5, Beclin-1, and LC3B in the neutrophils of each group. (**D**) Quantitative analysis of ATG5 in (**C**) (*n* = 3). (**E**) Quantitative analysis of Beclin-1 in (**C**) (*n* = 3). (**F**) Quantitative analysis of LC3B in (**C**) (*n* = 3). (**G**) IF analysis of the expression of LC3B in the neutrophils of each group. (**H**) Quantitative analysis of LC3B in (**G**) (*n* = 3). (**I**) Transmission electron microscopy results for each group. The Orange arrows indicate autophagosomes. The values are presented as the means ± SDs. **P*<0.05, ***P*<0.01.

IL-8, chemokines and adhesion molecules.[62] The PAD4-mediated citrullination of histone proteins is an important component of NETs. In murine sepsis models, Cl-amidine, a PAD inhibitor, inhibits NET formation and increases the survival rate.[63] In patients with relatively high levels of ACPAs, elevated levels of hypoxia-inducible factor 1α (HIF-1α) and PAD4 were observed, along with cellular protein citrullination.[64] SMS significantly inhibited PAD4 expression in mice with AA and in neutrophils, accompanied by decreased NET formation. The regulatory effect of PAD4 could result from compounds in the SMS decoction. Given that PAD4 is a promising target for RA intervention, some studies have been carried out to identify natural inhibitors of TCM.[65–67] Systematic analysis of the effective components of SMS deposits and their potential targets has also been conducted using advanced approaches that require thorough integration and validation.[31,34,40]

ROS exacerbate RA by activating immune cells, worsening inflammation, and inducing osteoclasts.[68] ROS also facilitate the formation of NETs.[69] Excessive accumulation of ROS disrupts cellular homeostasis, leading to oxidative stress, mitochondrial dysfunction, and the induction of autophagy.[70] In this study, SMS strongly suppressed ROS production in local joints in vivo and inhibited ROS production by neutrophils in vitro. However, the latest research on bone marrow-derived neutrophils in CIA mice using single-cell sequencing technology has proposed that ROS play bidirectional roles in different subsets of neutrophils during immune priming.[71] Neutrophil heterogeneity may also affect the roles of NETs formed by different disease subsets in diseases,[72] leaving more sophisticated questions for researchers to resolve.

The PI3K signalling pathway is one of the essential signalling pathways regulating cell growth, proliferation, motility, metabolism and survival.[73,74] Activation of the PI3K/AKT signalling pathway in neutrophils leads to ROS generation and NET formation.[75,76] The RA-related sleep deprivation likely exacerbates the oxidative stress, leading to the production of ROS and the activation of AKT signalling.[78] Inhibition of the PI3K/AKT signalling pathway has been reported to strongly alleviate RA by suppressing the excretion of inflammatory cytokines and delaying the apoptosis of fibroblasts,[79,80] which is consistent with our results. SMS can reduce ROS production and phosphorylation in the PI3K/AKT pathway both in vivo and in vitro.

This SMS decoction is a traditional prescription containing various ingredients. The active compounds remain to be investigated. Besides, how the autophagy contributes to NET formation is still confusing. As previously reported, the induction of apoptosis contributes to decreased autophagy and NET formation.[57,77] Further research is needed to elucidate these underlying mechanisms of SMS.

Conclusion

SMS offers the potential advantage over conventional therapies through multi-target regulatory mechanisms. Our study demonstrated that SMS had significant anti-inflammatory and immunomodulatory effects through the AKT/ROS/autophagy axis in an experimental RA model and in neutrophils.

Abbreviations

RA, rheumatoid arthritis; NETs, neutrophil extracellular traps; ACPAs, antibodies to citrullinated protein antigens; MPO, myeloperoxidase; NE, neutrophil elastase; PAD4, peptidyl arginine deiminase 4; CitH3, citrullinated histone H3; LC3B, microtubule-associated protein 1 light chain 3B; IL-6, interleukin-6; TNF-α, tumor necrosis factor-α; MTX, methotrexate; CIA, collagen-induced arthritis; HIF-1α, hypoxia-inducible factor-1α; AA, adjuvant-induced arthritis; PMA, phorbol 12-myristate 13-acetate; CBA, cytometric beads array; H&E staining, haematoxylin and eosin staining; IHC staining, immunohistochemistry staining; HRP, Horseradish Peroxidase; PAD4, protein arginine deiminase 4; DMARDs, disease-modifying antirheumatic drugs; PI3K, phosphatidylinositol-3-kinase; AKT, Protein Kinase B; TCM, traditional Chinese medicine; TEM, transmission electron microscopy; SCFAs, short-chain fatty acids; ROS, reactive oxygen species.

Data Sharing Statement

Data supporting the findings of this study will be made available upon reasonable request on Qingyi Lu (lu_qingyi@126.com).

Ethics Approval

This animal experiment was approved by the Animal Ethics Committee of Beijing University of Chinese Medicine (BUCM-2023031004-1027). All the experiments were performed and analysed in accordance with ARRIVE guidelines and guidelines for the ethical review of laboratory animal welfare (GB/T35892-2018) issued by China.

Acknowledgment

This work was supported by the National Natural Science Foundation of China (Grant Number: 82205068), Research Program of Beijing University of Chinese Medicine (Grant Number: 2023-JYB-JBQN-019), and NATCM's Project for

High-level Construction of Key TCM Disciplines-Beijing University of Chinese Medicine (Grant Number: zyyzdxk-2023262). Abstract graph was created with BioRender (BioRender Inc., California, United States).

Disclosure

The authors declare that they have no conflict of interest. All authors have read and agreed to the published version of the manuscript.

References

1. Wu D, Luo Y, Li T, et al. Systemic complications of rheumatoid arthritis: focus on pathogenesis and treatment. *Front Immunol*. 2022;13:1051082. doi:10.3389/fimmu.2022.1051082
2. Conforti A, Di Cola I, Pavlych V, et al. Beyond the joints, the extra-articular manifestations in rheumatoid arthritis. *Autoimmun Rev*. 2021;20(2):102735. doi:10.1016/j.autrev.2020.102735
3. Coskun Benlidayi I. Sleep impairment: an obstacle to achieve optimal quality of life in rheumatoid arthritis. *Rheumatol Int*. 2018;38(12):2183–2192. doi:10.1007/s00296-018-4155-5
4. Di Matteo A, Bathon JM, Emery P. Rheumatoid arthritis. *Lancet*. 2023;402(10416):2019–2033. doi:10.1016/S0140-6736(23)01525-8
5. Jiang Q, Wang X, Huang E, et al. Inflammasome and its therapeutic targeting in rheumatoid arthritis. *Front Immunol*. 2021;12:816839. doi:10.3389/fimmu.2021.816839
6. van Delft MAM, Huizinga TWJ. An overview of autoantibodies in rheumatoid arthritis. *J Autoimmun*. 2020;110:102392. doi:10.1016/j.jaut.2019.102392
7. Karmakar U, Vermeren S. Crosstalk between B cells and neutrophils in rheumatoid arthritis. *Immunology*. 2021;164(4):689–700. doi:10.1111/imm.13412
8. Jing W, Liu C, Su C, et al. Role of reactive oxygen species and mitochondrial damage in rheumatoid arthritis and targeted drugs. *Front Immunol*. 2023;14:1107670. doi:10.3389/fimmu.2023.1107670
9. Mutua V, Gershwin LJ. A review of neutrophil extracellular traps (NETs) in disease: potential Anti-NETs therapeutics. *Clin Rev Allergy Immunol*. 2021;61(2):194–211. doi:10.1007/s12016-020-08804-7
10. Skendros P, Mitroulis I, Ritis K. Autophagy in neutrophils: from granulopoiesis to neutrophil extracellular traps. *Front Cell Develop Biol*. 2018;6. doi:10.3389/fcell.2018.00006
11. Jorch SK, Kubes P. An emerging role for neutrophil extracellular traps in noninfectious disease. *Nat Med*. 2017;23(3):279–287. doi:10.1038/nm.4294
12. Guo Y, Gao F, Wang X, et al. Spontaneous formation of neutrophil extracellular traps is associated with autophagy. *Sci Rep*. 2021;11(1):24005. doi:10.1038/s41598-021-03520-4
13. Xu F, Zhang C, Zou Z, et al. Aging-related Atg5 defect impairs neutrophil extracellular traps formation. *Immunology*. 2017;151(4):417–432. doi:10.1111/imm.12740
14. Papayannopoulos V. Neutrophil extracellular traps in immunity and disease. *Nat RevImmunol*. 2018;18(2):134–147. doi:10.1038/nri.2017.105
15. Khanmohammadi M, Danish H, Sekar NC, et al. Cyclic stretch enhances neutrophil extracellular trap formation. *BMC Biol*. 2024;22(1):209. doi:10.1186/s12915-024-02009-6
16. Wang Y, Guo J, Zhang D, et al. IDH1/MDH1 deacetylation promotes NETosis by regulating OPA1 and autophagy. *Int Immunopharmacol*. 2024;143(Pt 1):113270. doi:10.1016/j.intimp.2024.113270
17. Malamud M, Whitehead L, McIntosh A, et al. Recognition and control of neutrophil extracellular trap formation by MICL. *Nature*. 2024;633(8029):442–450. doi:10.1038/s41586-024-07820-3
18. Smith MH, Berman JR. What is rheumatoid arthritis? *JAMA*. 2022;327(12):1194. doi:10.1001/jama.2022.0786
19. Emery P, Pope JE, Kruger K, et al. Efficacy of monotherapy with biologics and JAK inhibitors for the treatment of rheumatoid arthritis: a systematic review. *Adv Ther*. 2018;35(10):1535–1563. doi:10.1007/s12325-018-0757-2
20. Mahmoud EM, Radwan A, Elsayed SA. A prospective randomized-controlled non-blinded comparative study of the JAK inhibitor (baricitinib) with TNF-α inhibitors and conventional DMARDs in a sample of Egyptian rheumatoid arthritis patients. *Clin Rheumatol*. 2024;43(12):3657–3668. doi:10.1007/s10067-024-07194-x
21. Greenblatt HK, Kim H-A, Bettner LF, et al. Preclinical rheumatoid arthritis and rheumatoid arthritis prevention. *Curr Opin Rheumatol*. 2020;32(3):289–296. doi:10.1097/BOR.0000000000000708
22. Shi J, van de Stadt LA, Levarht EWN, et al. Anti-carbamylated protein (anti-CarP) antibodies precede the onset of rheumatoid arthritis. *Ann Rheum Dis*. 2014;73(4):780–783. doi:10.1136/annrheumdis-2013-204154
23. Cope AP, Jasenecova M, Vasconcelos JC, et al. Abatacept in individuals at high risk of rheumatoid arthritis (APIPPRA): a randomised, double-blind, multicentre, parallel, placebo-controlled, phase 2b clinical trial. *Lancet*. 2024;403(10429):838–849. doi:10.1016/S0140-6736(23)02649-1
24. Rech J, Tascilar K, Hagen M, et al. Abatacept inhibits inflammation and onset of rheumatoid arthritis in individuals at high risk (ARIAA): a randomised, international, multicentre, double-blind, placebo-controlled trial. *Lancet*. 2024;403(10429):850–859. doi:10.1016/S0140-6736(23)02650-8
25. Liang Y, Liu M, Cheng Y, et al. Prevention and treatment of rheumatoid arthritis through traditional Chinese medicine: role of the gut microbiota. *Front Immunol*. 2023;14:1233994. doi:10.3389/fimmu.2023.1233994
26. Kong XY, Wen CP. On research progress of western and Chinese medicine treatment on pre-rheumatoid arthritis. *Chin J Integr Med*. 2019;25(9):643–647. doi:10.1007/s11655-019-3223-3
27. Peng J, Lu X, Xie K, et al. Dynamic alterations in the gut microbiota of collagen-induced arthritis rats following the prolonged administration of total glucosides of paeony. *Front Cell Infect Microbiol*. 2019;9:204. doi:10.3389/fcimb.2019.00204
28. Fan Z, Yang B, Ross RP, et al. The prophylactic effects of different Lactobacilli on collagen-induced arthritis in rats. *Food Funct*. 2020;11(4):3681–3694. doi:10.1039/C9FO02556A

29. Yang Y, Hong Q, Zhang X, et al. Rheumatoid arthritis and the intestinal microbiome: probiotics as a potential therapy. *Front Immunol*. 2024;15:1331486. doi:10.3389/fimmu.2024.1331486
30. Liu H, Kong L, Cao D, et al. Efficacy and mechanism of the Ermiao San series of formulas for rheumatoid arthritis based on Chinmedomics strategy. *Phytomedicine*. 2024;132:155903. doi:10.1016/j.phymed.2024.155903
31. Wang Y, Zhang F, Li X, et al. Integrated multi-omics techniques and network pharmacology analysis to explore the material basis and mechanism of simiao pill in the treatment of rheumatoid arthritis. *ACS Omega*. 2023;8(12):11138–11150. doi:10.1021/acsomega.2c07959
32. Shen P, Huang Y, Ba X, et al. Si miao san attenuates inflammation and oxidative stress in rats with CIA via the modulation of the Nrf2/ARE/PTEN pathway. *Evid Based Complement Alternat Med*. 2021;2021:2843623. doi:10.1155/2021/2843623
33. Ba X, Wang H, Huang Y, et al. Simiao pill attenuates collagen-induced arthritis and bleomycin-induced pulmonary fibrosis in mice by suppressing the JAK2/STAT3 and TGF-β/Smad2/3 signalling pathway. *J Ethnopharmacol*. 2023;309:116274. doi:10.1016/j.jep.2023.116274
34. Chen Y, Liu H, Han R, et al. Analyzing how SiMiao Wan regulates ferroptosis to prevent RA-ILD using metabolomics and cyberpharmacology. *Phytomedicine*. 2024;133:155912. doi:10.1016/j.phymed.2024.155912
35. Jiang H, Lu Q, Xu J, et al. Sinomenine ameliorates adjuvant-induced arthritis by inhibiting the autophagy/NETosis/inflammation axis. *Scientific Rep*. 2023;13(1):3933. doi:10.1038/s41598-023-30922-3
36. Zheng J, Hu J, Yang Y, et al. Suppressive effect of Tripterygium hypoglaucum (Levl.) Hutch extract on rheumatoid arthritis in mice by modulating inflammasome and bile acid metabolism. *Biomed Pharmacother*. 2023;167:115494. doi:10.1016/j.biopha.2023.115494
37. Svensson MND, Zoccheddu M, Yang S, et al. Synoviocyte-targeted therapy synergizes with TNF inhibition in arthritis reversal. *Sci Adv*. 2020;6 (26):eaba4353. doi:10.1126/sciadv.aba4353
38. Yuan K, Zhu Q, Lu Q, et al. Quercetin alleviates rheumatoid arthritis by inhibiting neutrophil inflammatory activities. *J Nutr Biochem*. 2020;84:108454. doi:10.1016/j.jnutbio.2020.108454
39. Lu Q, Yuan K, Li X, et al. Detecting migration and infiltration of neutrophils in mice. *J Vis Exp*. 2020;6(156):e60543.
40. Zeng L, Deng Y, Zhou X, et al. Simiao pills alleviates renal injury associated with hyperuricemia: a multi-omics analysis. *J Ethnopharmacol*. 2024;333:118492. doi:10.1016/j.jep.2024.118492
41. Peng X, Zou Q, Yang C, et al. Unveiling the multifaceted benefits of Simiao Pill in ulcerative colitis: integrative analysis of signaling pathways, gut microbiota, and lipid metabolism. *J Ethnopharmacol*. 2025;346:119714. doi:10.1016/j.jep.2025.119714
42. Xin L, Feng H-C, Zhang Q, et al. Exploring the osteogenic effects of simiao wan through activation of the PI3K/AKT pathway in osteoblasts. *J Ethnopharmacol*. 2025;338:119023. doi:10.1016/j.jep.2024.119023
43. O'Neil LJ, Kaplan MJ. Neutrophils in rheumatoid arthritis: breaking immune tolerance and fueling disease. *Trends Mol Med*. 2019;25(3):215–227. doi:10.1016/j.molmed.2018.12.008
44. Lee KH, Kronbichler A, Park DD-Y, et al. Neutrophil extracellular traps (NETs) in autoimmune diseases: a comprehensive review. *Autoimmun Rev*. 2017;16(11):1160–1173. doi:10.1016/j.autrev.2017.09.012
45. Wright HL, Lyon M, Chapman EA, et al. Rheumatoid arthritis synovial fluid neutrophils drive inflammation through production of chemokines, reactive oxygen species, and neutrophil extracellular traps. *Front Immunol*. 2020;11:584116. doi:10.3389/fimmu.2020.584116
46. Fousert E, Toes R, Desai J. Neutrophil extracellular traps (NETs) take the central stage in driving autoimmune responses. *Cells*. 2020;9(4):915. doi:10.3390/cells9040915
47. Lin X, Shao T, Huang L, et al. Simiao decoction alleviates gouty arthritis by modulating proinflammatory cytokines and the gut ecosystem. *Front Pharmacol*. 2020;11:955. doi:10.3389/fphar.2020.00955
48. Azzouz D, Khan MA, Palaniyar N. ROS induces NETosis by oxidizing DNA and initiating DNA repair. *Cell Death Discov*. 2021;7(1):113. doi:10.1038/s41420-021-00491-3
49. Hu Y, Wang H, Liu Y. NETosis: Sculpting tumor metastasis and immunotherapy. *Immunol Rev*. 2024;321(1):263–279. doi:10.1111/imr.13277
50. Lou X, Chen H, Chen S, et al. LL37 / FPR2 regulates neutrophil mPTP promoting the development of neutrophil extracellular traps in diabetic retinopathy. *FASEB J*. 2024;38(11):e23697. doi:10.1096/fj.202400656R
51. Oliveira JSS, Santos GDS, Moraes JA, et al. Reactive oxygen species generation mediated by NADPH oxidase and PI3K/Akt pathways contribute to invasion of Streptococcus agalactiae in human endothelial cells. *Mem Inst Oswaldo Cruz*. 2018;113(6):e140421. doi:10.1590/0074-02760170421
52. Dan Dunn J, Alvarez LA, Zhang X, et al. Reactive oxygen species and mitochondria: a nexus of cellular homeostasis. *Redox Biol*. 2015;6:472–485. doi:10.1016/j.redox.2015.09.005
53. An Q, Yan W, Zhao Y, et al. Enhanced neutrophil autophagy and increased concentrations of IL-6, IL-8, IL-10 and MCP-1 in rheumatoid arthritis. *Int Immunopharmacol*. 2018;65:119–128. doi:10.1016/j.intimp.2018.09.011
54. Vomero M, Manganelli V, Barbati C, et al. Reduction of autophagy and increase in apoptosis correlates with a favorable clinical outcome in patients with rheumatoid arthritis treated with anti-TNF drugs. *Arthritis Res Ther*. 2019;21(1):39. doi:10.1186/s13075-019-1818-x
55. Bhattacharya A, Wei Q, Shin J, et al. Autophagy is required for neutrophil-mediated inflammation. *Cell Rep*. 2015;12(11):1731–1739. doi:10.1016/j.celrep.2015.08.019
56. Wang S, Zheng S, Zhang Q, et al. Atrazine hinders PMA-induced neutrophil extracellular traps in carp via the promotion of apoptosis and inhibition of ROS burst, autophagy and glycolysis. *Environ Pollut*. 2018;243(Pt A):282–291. doi:10.1016/j.envpol.2018.08.070
57. Li X, Yuan K, Zhu Q, et al. Andrographolide ameliorates rheumatoid arthritis by regulating the apoptosis-NETosis balance of neutrophils. *Int J Mol Sci*. 2019;20(20):5035. doi:10.3390/ijms20205035
58. Douda DN, Yip L, Khan MA, et al. Akt is essential to induce NADPH-dependent NETosis and to switch the neutrophil death to apoptosis. *Blood*. 2014;123(4):597–600. doi:10.1182/blood-2013-09-526707
59. van der Linden M, Westerlaken GHA, van der Vlist M, et al. Differential signalling and kinetics of neutrophil extracellular trap release revealed by quantitative live imaging. *Sci Rep*. 2017;7(1):6529. doi:10.1038/s41598-017-06901-w
60. Remijsen Q, Berghe TV, Wirawan E, et al. Neutrophil extracellular trap cell death requires both autophagy and superoxide generation. *Cell Res*. 2011;21(2):290–304. doi:10.1038/cr.2010.150
61. Xin L, Feng H-C, Zhang Q, et al. Exploring the osteogenic effects of Simiao Wan through activation of the PI3K/AKT pathway in osteoblasts. *J Ethnopharmacol*. 2024;338:119023.
62. Khandpur R, Carmona-Rivera C, Vivekanandan-Giri A, et al. NETs are a source of citrullinated autoantigens and stimulate inflammatory responses in rheumatoid arthritis. *Sci Transl Med*. 2013;5(178):178ra40. doi:10.1126/scitranslmed.3005580

63. Biron BM, Chung C-S, O'Brien XM, et al. Cl-amidine prevents histone 3 citrullination and neutrophil extracellular trap formation, and improves survival in a murine sepsis model. *J Innate Immun*. 2017;9(1):22–32. doi:10.1159/000448808
64. Wu H, Yuan H, Zhang J, et al. Helicobacter pylori upregulates PAD4 expression via stabilising HIF-1α to exacerbate rheumatoid arthritis. *Ann Rheum Dis*. 2024;83(12):1666–1676. doi:10.1136/ard-2023-225306
65. Zhao J, Li Y, Gao C, et al. Screening of natural inhibitors against peptidyl arginine deiminase 4 from herbal extracts by a high-performance liquid chromatography ultraviolet-visible based method. *J Chromatogr A*. 2024;1716:464643. doi:10.1016/j.chroma.2024.464643
66. Zhao J, Zhang S, Dong J, et al. Screening and identification of peptidyl arginine deiminase 4 inhibitors from herbal plants extracts and purified natural products by a trypsin assisted sensitive immunoassay based on streptavidin magnetic beads. *Talanta*. 2024;279:126611. doi:10.1016/j.talanta.2024.126611
67. Zhao Z, Wang C, Zhao J, et al. Immobilized PAD4 enzyme on magnetic nanoparticles for screening natural inhibitors from traditional Chinese medicines. *Talanta*. 2024;278:126492. doi:10.1016/j.talanta.2024.126492
68. Jeon S, Min Kim T, Kwon G, et al. Targeting ROS in osteoclasts within the OA environment: a novel therapeutic strategy for osteoarthritis management. *J Tissue Eng*. 2024;15:20417314241279935. doi:10.1177/20417314241279935
69. Douda DN, Khan MA, Grasemann H, et al. SK3 channel and mitochondrial ROS mediate NADPH oxidase-independent NETosis induced by calcium influx. *Proc Natl Acad Sci U S A*. 2015;112(9):2817–2822. doi:10.1073/pnas.1414055112
70. Li L, Tan J, Miao Y, et al. ROS and autophagy: interactions and molecular regulatory mechanisms. *Cell Mol Neurobiol*. 2015;35(5):615–621. doi:10.1007/s10571-015-0166-x
71. Chen T, Zhou Z, Liu Y, et al. Neutrophils with low production of reactive oxygen species are activated during immune priming and promote development of arthritis. *Redox Biol*. 2024;78:103401. doi:10.1016/j.redox.2024.103401
72. Sollberger G, Tilley DO, Zychlinsky A. Neutrophil extracellular traps: the biology of chromatin externalization. *Dev Cell*. 2018;44(5):542–553. doi:10.1016/j.devcel.2018.01.019
73. Yang J, Nie J, Ma X, et al. Targeting PI3K in cancer: mechanisms and advances in clinical trials. *Mol Cancer*. 2019;18(1):26. doi:10.1186/s12943-019-0954-x
74. Wang J, Hu K, Cai X, et al. Targeting PI3K/AKT signaling for treatment of idiopathic pulmonary fibrosis. *Acta Pharm Sin B*. 2022;12(1):18–32. doi:10.1016/j.apsb.2021.07.023
75. Zha C, Meng X, Li L, et al. Neutrophil extracellular traps mediate the crosstalk between glioma progression and the tumor microenvironment via the HMGB1/RAGE/IL-8 axis. *Cancer Biol Med*. 2020;17(1):154–168. doi:10.20892/j.issn.2095-3941.2019.0353
76. Muraro SP, De Souza GF, Gallo SW, et al. Respiratory syncytial virus induces the classical ROS-dependent NETosis through PAD-4 and necroptosis pathways activation. *Sci Rep*. 2018;8(1):14166. doi:10.1038/s41598-018-32576-y
77. Jiang H, Lu Q, Huang X, et al. Sinomenine-glycyrrhizic acid self-assembly enhanced the anti-inflammatory effect of sinomenine in the treatment of rheumatoid arthritis. *J Controlled Release*. 2025;382:113718. doi:10.1016/j.jconrel.2025.113718
78. Li Y, Zhang Y, Ji G, et al. Autophagy triggered by oxidative stress appears to be mediated by the AKT/mTOR signaling pathway in the liver of sleep-deprived rats. *Oxidative Med Cell Longevity*. 2020;2020(1):6181630. doi:10.1155/2020/6181630
79. Jia Q, Che Q, Zhang X, et al. Knockdown of Galectin-9 alleviates rheumatoid arthritis through suppressing TNF-α-induced activation of fibroblast-like synoviocytes. *Biochem Pharmacol*. 2024;220:115994. doi:10.1016/j.bcp.2023.115994
80. Liu Q, Wang J, Ding C, et al. Sinomenine alleviates rheumatoid arthritis by suppressing the PI3K-Akt signaling pathway, as demonstrated through network pharmacology, molecular docking, and experimental validation. *Drug Des Devel Ther*. 2024;18:3523–3545. doi:10.2147/DDDT.S475959